Mixtures of *n*-Octyl-*β*-D-glucoside and Triethylene Glycol Mono-*n*-octyl Ether: Phase Behavior and Micellar Structure near the Liquid−Liquid Phase Boundary†

Gabriella M. Santonicola and Eric W. Kaler*

Center for Molecular and Engineering Thermodynamics, Department of Chemical Engineering, University of Delaware, Newark, Delaware 19716

Received March 2, 2005. In Final Form: July 19, 2005

The phase behavior and microstructure of aqueous mixtures of *n*-octyl-*β*-D-glucoside ($C_8\beta G_1$) and triethylene glycol mono-*n*-octyl ether (C_8E_3) is presented. $C_8\beta G_1$ forms a one-phase micellar solution in water at surfactant concentrations up to 60 wt %, whereas mixtures with C_8E_3 show a liquid−liquid phase transition at low surfactant concentration. The position of this phase boundary for mixtures can be rationally shifted in the temperature−composition window by altering the ratio of the two surfactants. Small-angle neutron scattering is used to determine the size and shape of the mixed micelles and to characterize the nature of the fluctuations near the cloud point of the micellar solutions. The $C_8\beta G_1/C_8E_3$ solutions are characterized by concentration fluctuations that become progressively stronger upon approach to the liquid−liquid phase boundary, whereas micellar growth is negligible. Such observations confirm previous views of the role of the surfactant phase boundary in tuning attractive micellar interactions, which can be used effectively to change the nature and strength of interparticle interactions in colloidal dispersions. Colloidal silica particles were then added to these surfactant mixtures and were found to aggregate at conditions near the cloud point. This finding is relevant to current strategies for protein crystallization.

Introduction

Surfactants are effectively used to alter the macroscopic behavior of solid dispersions in solution. In particular, there is a well-accepted observation that properties of solutions in the proximity of surfactant phase boundaries may help promote aggregation in colloid and protein solutions. Furthermore, charged polystyrene particles form crystalline structures near the surfactant-rich side of the phase boundary of *n*-alkyl polyglycol ethers (C_iE_j) in water.[1] Similarly, Garavito observed that membrane protein crystallization, which occurs in surfactant solutions that solubilize these proteins, is affected by the presence of the surfactant phase boundary and that well-ordered crystals are often grown in the proximity of such boundaries.[2] However, determining the extent of the region "near the phase boundary" and elucidating the kinds of interactions active there is an open question.

In surfactant solutions, tuning of micellar interactions can be accomplished by adding one or more of several agents. Among these, the most commonly used are salts, polymers, and other surfactants. The addition of salt often has an effect on the size of the micelles and usually leads to micellar growth or elongation. This may be detrimental in applications involving membrane proteins, where their functionality outside biological membranes depends on the micellar packing around the hydrophobic core. Salt addition may also lead to poorly ordered crystals. The addition of a second surfactant also leads to a wide variety of often unpredictable behavior. In many cases, mixtures of surfactants show synergism and as a result have been extensively studied.[3−6]

To understand the effect of surfactant solutions on colloidal dispersions, it is important to characterize the phase behavior and the microstructure of such solutions. Both the strength and the range of the concentration fluctuations driven by the attractive intermicellar interactions are crucial in promoting colloid aggregation. Small-angle neutron scattering is a powerful technique to elucidate the microstructure of colloidal aggregates in solution. Small-angle scattering data can be analyzed by using the indirect Fourier transformation (IFT) method,[7] and its extension to interacting particles, the generalized indirect Fourier transformation (GIFT), which in some cases allows separation of information about the geometry and the interactions of the aggregates.[8]

Here we investigate the phase behavior and microstructure of aqueous mixtures of *n*-octyl-*β*-D-glucoside ($C_8\beta G_1$) and triethylene glycol mono-*n*-octyl ether (C_8E_3). $C_8\beta G_1$ belongs to the family of alkyl-polyglucoside surfactants and has been extensively used in processes involving biological macromolecules because of its nonionic and nontoxic nature. Its amphiphilic balance is highly effective in extracting membrane proteins from biological membranes with minimal impact on the native protein structure. Because of the relatively short carbon chain, $C_8\beta G_1$ does not show a Krafft boundary, below which surfactant molecules precipitate, and is completely miscible with water at all temperatures and at all concentrations up to 60 wt %.[9] However, C_8E_3 in water forms a lower consolute phase boundary with a critical point of

† Part of the Bob Rowell Festschrift special issue.

* To whom correspondence should be addressed. E-mail: kaler@che.udel.edu. Tel: (302) 831-3553. Fax: (302) 831-6751.

(1) Koehler, R. D.; Kaler, E. W. *Langmuir* **1997**, *13*, 2463−2470.
(2) Garavito, R. M.; Markovic-Housley, Z.; Jenkins, J. A. *J. Cryst. Growth* **1986**, *76*, 701−709.
(3) Ogino, K.; Abe, M. *Mixed Surfactant Systems*; Marcel Dekker: New York, 1992; Vol. 46.
(4) Laughlin, R. *The Aqueous Phase Behavior of Surfactants*; Academic Press: New York, 1994.
(5) Khan, A.; Marques, E. F. *Curr. Opin. Colloid Interface Sci.* **1999**, *4*, 402−410.
(6) Kronberg, B. *Curr. Opin. Colloid Interface Sci.* **1997**, *2*, 456−463.
(7) Glatter, O. *J. Appl. Crystallogr.* **1977**, *10*, 415−421.
(8) Brunner-Popela, J.; Glatter, O. *J. Appl. Crystallogr.* **1997**, *30*, 431−442.
(9) Nilsson, F.; Soderman, O.; Johansson, I. *Langmuir* **1996**, *12*, 902−908.

10.1021/la050573v CCC: $30.25
Published on Web 08/23/2005

about 8 °C.[10−12] Solutions of C_iE_j surfactants in water exhibit strong concentration fluctuations that extend for a wide temperature range below the critical temperature.[10,13] Furthermore, for C_iE_j molecules with short hydrophobic chains negligible micellar growth has been observed upon increasing temperature.[13,14] In this work, the addition of C_8E_3 is proposed as an effective way to tune micellar interactions in mixtures with $C_8\beta G_1$ without significant micellar elongation. Properties of the mixed micelles of these two surfactants are studied at solution conditions close to the liquid−liquid phase boundary by means of small-angle neutron scattering. The geometrical features of the micelles and the interactions in such solutions are characterized in view of their fundamental role in the macroscopic behavior of colloidal dispersions.

Experimental Methods

Materials. *n*-Octyl-β-D-glucoside ($C_8\beta G_1$) (Anagrade, purity >99%) was purchased from Anatrace Inc. (Maumee, OH) and used without further purification because it displayed a sharp cmc break. Triethylene glycol mono-*n*-octyl ether (C_8E_3) was obtained from Sigma-Aldrich Co. (St. Louis, MO), and its purity was verified by NMR and mass spectroscopy. Deuterium oxide (DLM-11, 99.9% deuterated, low paramagnetic) was obtained from Cambridge Isotope Laboratories Inc. (Andover, MA) and used as received. Sodium chloride and sodium phosphate were purchased from Sigma-Aldrich Co. Colloidal silica particles (Ludox TM-50, 50 wt % suspension in water, pH 9) were purchased from Sigma-Aldrich Co. The average particle size reported by the manufacturer was 22 nm.

Phase Behavior. The phase behavior of ternary mixtures of water, $C_8\beta G_1$, and C_8E_3 was studied at constant pressure by varying three independent variables: the temperature T, the mass fraction of total surfactant in solution (γ), defined as

$$\gamma = \frac{C_8E_3 + C_8\beta G_1}{C_8E_3 + C_8\beta G_1 + H_2O} \quad (1)$$

and the mass ratio of C_8E_3 to the total surfactant in the mixture (δ), defined as

$$\delta = \frac{C_8E_3}{C_8\beta G_1 + C_8E_3} \quad (2)$$

Samples were prepared by weight by dilution of stock solutions. Stock solutions were deoxygenated with argon to prevent degradation of the ethoxylate groups of C_8E_3. Millipore deionized water was used to prepare surfactant solutions. Samples were left to equilibrate in a water bath stable to ±0.1 °C from a minimum of 24 h up to 1 week, depending on the concentration. Phase diagrams were mapped out by direct visual inspection of the samples. Cloud points were determined with an accuracy of ±0.05 °C, unless otherwise stated. Samples were examined by crossed light polarizers for homogeneity and birefringence.

Surface Tension Measurements. Critical micelle concentrations were determined by analysis of plots of surface tension versus concentration. A Kruss K-10 model tensiometer with a Wilhelmy plate was used to measure the surface tension. Solutions were equilibrated for 24 h in a water bath at the temperature chosen for the experiment and then for 30 min in the sample holder of the tensiometer before taking each measurement.

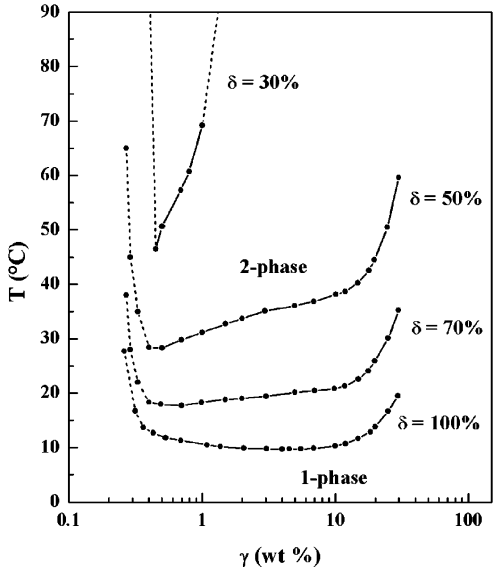

Figure 1. Pseudobinary phase diagram of aqueous mixtures of $C_8\beta G_1$ and C_8E_3 with varying δ. Dotted lines are representative of samples that remained visibly turbid after several weeks.

Small-Angle Neutron Scattering. Small-angle neutron scattering experiments were performed at the Center for High-Resolution Neutron Scattering of the National Institute of Standards and Technology (NIST) in Gaithersburg, MD. In SANS experiments, the orientation-averaged intensities of neutrons scattered by particles in solution are measured as a function of the magnitude of the scattering vector, $q = (4\pi/\lambda)\sin(\theta/2)$, where θ is the angle between the scattered and incident beams. Here the average neutron wavelength was 6 Å, with a spread $\Delta\lambda/\lambda$ of 15%. Data were collected on the NG-3 instrument at sample−detector distances of 1.33, 4.5, and 13 m covering a q range of 0.004 to 0.5 $Å^{-1}$ (with the detector offset of 25 cm from the center at the shortest distances). Samples were held in quartz cells of 2 mm optical path length and left to equilibrate at the temperature of interest before being transferred to the temperature-controlled sample chamber. The acidity of buffer solutions in D_2O was measured with a glass electrode and corrected by adding 0.4 units to take into account the difference in the pH meter reading between H_2O and D_2O solutions.[15] The raw scattering data were corrected for solvent, empty cell, and buffer solution scattering, all measured separately, and placed on an absolute scale using standards calibrated by NIST.

Static Light Scattering. Experiments were performed on a Brookhaven light scattering apparatus equipped with a 200SM goniometer. The wavelength of the light was 488 nm from an Ar^- ion laser (Lexel 95). The sample was held in a temperature-controlled cell. Scattering intensities were collected at angles from 30 to 120° corresponding to a q range of 0.0009 to 0.003 $Å^{-1}$. Benzene was used as a reference solvent to place the scattered intensities on an absolute scale.[16] All refractive indices were measured by a differential refractometer (C. N. Wood, RF-600) using a wavelength filter.

Results and Discussion

Phase Behavior of $C_8\beta G_1/C_8E_3/H_2O$ Mixtures. Figure 1 shows the pseudobinary phase diagram of $C_8\beta G_1/C_8E_3/H_2O$ mixtures for total surfactant concentrations (γ) ranging from 0 to 30 wt % and for δ = 30, 50, 70, and 100%. The binary system $C_8\beta G_1/H_2O$ ($\delta = 0$) is characterized by an isotropic micellar phase that extends to a concentration of 60 wt % $C_8\beta G_1$ and on the entire temperature scale up to 100 °C.[9] Upon addition of C_8E_3 to the $C_8\beta G_1/H_2O$ system, a lower consolute boundary forms for γ in the range of 0 to 30 wt %. The two-phase

(10) Mitchell, D. J.; Tiddy, G. J. T.; Waring, L.; Bostock, T.; McDonald, M. P. *J. Chem. Soc., Faraday* Trans. **1983**, *79*, 975−1000.
(11) Corkill, J. M.; Goodman, J. F.; Harrold, S. P. *Trans. Faraday Soc.* **1964**, *60*, 202.
(12) Schubert, K. V.; Kaler, E. W. *Ber. Bunsen-Ges. Phys. Chem.* **1996**, *100*, 190−205.
(13) Zulauf, M.; Rosenbusch, J. P. *J. Phys. Chem.* **1983**, *87*, 856−862.
(14) Zulauf, M.; Weckstrom, K.; Hayter, J. B.; Degiorgio, V.; Corti, M. *J. Phys. Chem.* **1985**, *89*, 3411−3417.
(15) Glasoe, P. K.; Long, F. A. *J. Phys. Chem.* **1960**, *64*, 188−190.
(16) Chu, B. *Laser Light Scattering*; Academic Press: Boston, 1991.

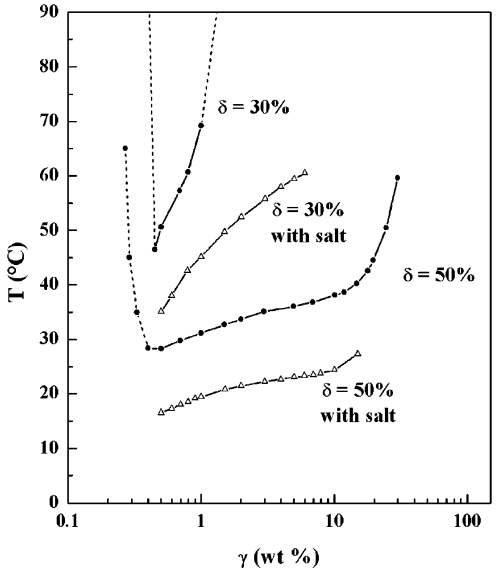

Figure 2. Phase boundaries of $C_8\beta G_1/C_8E_3$ mixtures in water ($C_8\beta G_1/C_8E_3$) and in buffer solution with 0.5 M NaCl and 0.1 M sodium phosphate at pH 6.5 (△).

region in the ternary mixture shifts to lower temperatures with increasing δ and becomes wider until it merges into the C_8E_3/H_2O ($\delta = 100\%$) miscibility gap. The lower cloud points T_β were determined to be 46.5, 28.3, 17.7, and 8.0 °C for $\delta = 30$, 50, 70, and 100%, respectively. No samples were birefringent, so there are no hexagonal or lamellar liquid crystalline phases present in the concentration ranges examined. Mixtures with a surfactant concentration below 0.5 wt % show some degree of haziness for a temperature range of 10 to 15 °C below the transition point. This phenomenon is probably due to the presence of water-insoluble impurities that precipitate as the surfactant concentration decreases below the critical micelle concentration (cmc).[17] Samples in the dilute micellar region (0.2−0.5 wt %) were left to equilibrate at each temperature for up to 1 week before phase observation. For γ above 20 wt %, the samples are viscous and phase separate slowly, but usually over 1 day. To rule out the presence of a cubic phase, the refractive index of $C_8\beta G_1/C_8E_3/H_2O$ mixtures in the concentration range from 0 to 30 wt % with $\delta = 50\%$ was measured at 25 °C. The refractive index varied smoothly with γ, so there is not a micellar-to-cubic phase transition below $\gamma = 30$ wt %.

The phase behavior of some $C_8\beta G_1/C_8E_3$ mixtures was also studied in a buffer solution at pH 6.5 and salt concentrations of 0.5 M NaCl and 0.1 M Na_2HPO_4/NaH_2PO_4 (on a surfactant-free basis). Salt effects in solutions of ethoxylate surfactants are generally limited compared to those in solutions of alkyl polyglucosides, and relatively high electrolyte concentrations are required to affect the cloud points.[18] Indeed, in the case of $C_8\beta G_1/C_8E_3$ mixtures we found that large shifts in the transition temperature occur when the mixtures are richer in the glucoside component. Solutions of pure C_8E_3 ($\delta = 100\%$) in a buffer with 0.5 M NaCl show a shift in the cloud temperature of about 3−5 °C. In mixtures with equal amounts of the two surfactants ($\delta = 50\%$), the phase-transition temperature shifts downward by about 10 °C (Figure 2) for a wide range of total surfactant concentration (0.5−15 wt %). For mixtures enriched in the glucoside component, as for $\delta = 30\%$ in Figure 2, the temperature shift is much larger and highly variable with surfactant concentration.

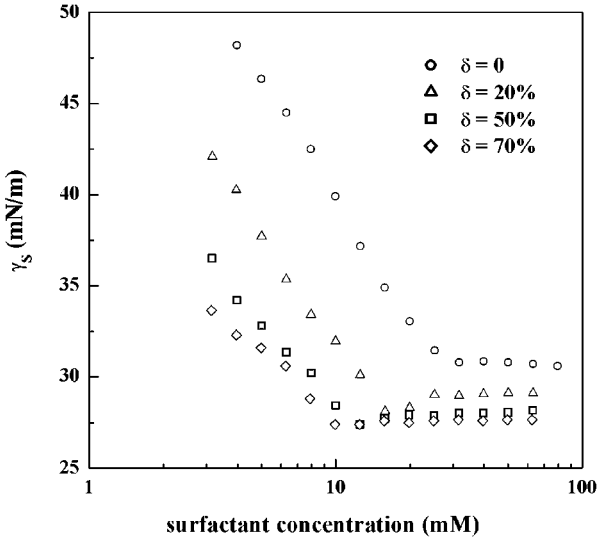

Figure 3. Surface tension γ_s vs total surfactant concentration for mixtures of $C_8\beta G_1$ and C_8E_3 with $\delta = 0$, 20, 50, and 70% in water at a temperature of 15 °C.

Micellization in $C_8\beta G_1/C_8E_3/H_2O$ Mixtures. Figure 3 shows plots of the equilibrium surface tension γ_s as a function of the total surfactant concentration for mixtures of $C_8\beta G_1$ and C_8E_3 in water with $\delta = 0$, 20, 50, and 70%. All measurements were carried out at 15 °C. The critical micelle concentrations (cmc) of these mixtures were determined to be the concentration at the intersection of the linear regions above and below the discontinuity in the plots. The critical micelle concentrations of the mixtures are 25.7, 14.4, 11.3, and 9.8 mM for $\delta = 0$, 20, 50, and 70% respectively. For pure C_8E_3 in water ($\delta = 100\%$), the value of 9.3 mM reported in the literature was used.[11]

Mixed surfactant systems are usually modeled using a pseudophase separation approach that is based on the assumption that the mixed micelles form a separate phase in equilibrium with the surfactant monomers.[19] According to this model, for binary surfactant systems the cmc of the mixture (cmc_{mix}) can be related to the cmc's and the activity coefficients of the pure surfactants by

$$\frac{1}{\mathrm{cmc}_{\mathrm{mix}}} = \frac{x_1}{f_1\mathrm{cmc}_1} + \frac{(1-x_1)}{f_2\mathrm{cmc}_2} \tag{3}$$

where x_1 is the bulk molar fraction of surfactant 1 in the surfactant mixture and f_1 and f_2 are the activity coefficients of the surfactants in the mixed micelle. If the two surfactants mix ideally, then the activity coefficients are unity, and the cmc's of mixtures can be predicted given the cmc's of the pure surfactants. When the mixing is nonideal, the activity coefficients can be described by the regular solution approximation.[20] In the regular solution approximation, the activity coefficients of the surfactants in the mixture are related to the surfactant composition of the mixed micelle by

$$f_1 = \exp \beta(1 - x_1^{\mathrm{mic}})^2 \tag{4}$$

$$f_2 = \exp \beta(x_1^{\mathrm{mic}})^2 \tag{5}$$

(17) Phillips, J. N.; Mysels, K. J. *J. Phys. Chem.* **1955**, *59*, 325−330.
(18) Balzer, D. In *Nonionic Surfactants: Alkyl Polyglucosides*; Balzer, D., Luders, H., Eds.; Marcel Dekker: New York, 2000; Vol. 91.
(19) Rubingh, D. N. In *Solution Chemistry of Surfactants*; Mittal, K. L., Ed.; Plenum Press: New York, 1979; Vol. 1.
(20) Scamehorn, J. F., Ed. *Phenomena in Mixed Surfactant Systems*; American Chemical Society: Washington, DC, 1986; Vol. 311.

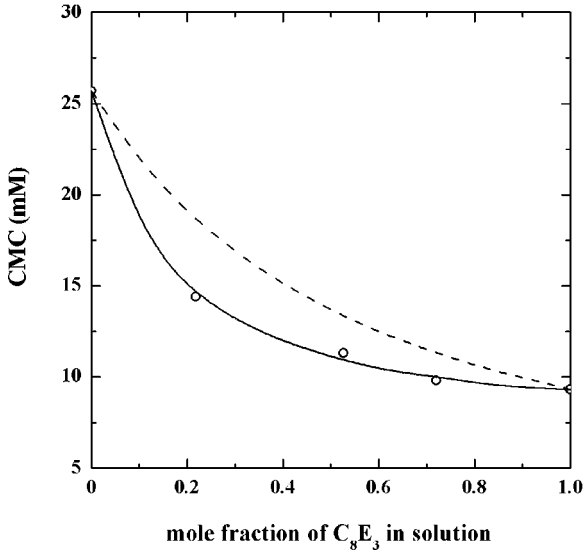

Figure 4. Critical micelle concentrations of mixtures of $C_8\beta G_1$ and C_8E_3 in water at 15 °C. The plotted points are experimental results, the dashed line is the theoretical prediction for ideal mixing, and the solid line is the fit of regular solution theory with $\beta = -1.0$.

where β is a parameter representing the net interaction between the surfactant monomers in the micelle and x_1^{mic} is the molar fraction of surfactant 1 in the mixed micelle. For nonionic/nonionic binary surfactant mixtures, the β parameter is usually slightly negative ($-1 < \beta \leq 0$), indicating weak interaction of the surfactant species in the mixture, and it is more negative ($-5 \leq \beta \leq -1$) for cationic/nonionic and anionic/nonionic mixtures because of electrostatic and solvation effects.[21] The value of β was determined by fitting eq 1 to the experimentally measured cmc value of mixtures at four different bulk compositions. The average value of β was -1.0 with a standard deviation of 0.1. Once the activity coefficients are known from the iterative fitting procedure, the mixed micelle composition (x_1^{mic}) at the cmc can be calculated from

$$x_1^{mic} = \frac{x_1 f_2 \mathrm{cmc}_2}{x_1 f_2 \mathrm{cmc}_2 + (1 - x_1) f_1 \mathrm{cmc}_1} \tag{6}$$

Figure 4 shows both the measured and the fitted values of cmc's for mixtures of $C_8\beta G_1$ and C_8E_3 in water at 15 °C as function of the molar fraction of C_8E_3 in solution. The dashed line represents the cmc's of the mixture in the ideal model ($\beta = 0$), whereas the solid line corresponds to the fit of the nonideal regular solution model with $\beta = -1.0$. Interactions in $C_8\beta G_1/C_8E_3$ aqueous mixtures are thus slightly stronger than what would be normally expected for nonionic/nonionic surfactant mixtures. The two surfactants have the same hydrophobic chain, so the nonideal behavior must result from the unlike hydrophilic headgroups and their interactions with water.

The mixed micelle composition at the cmc, as determined from regular solution theory with $\beta = -1.0$, varies as a function of the mass fraction of C_8E_3 in the total surfactant in solution (Figure 5). For all mixtures, the mixed micelles are richer in the component with the lower cmc, which is C_8E_3. There is an azeotrope with respect to the ideal mixing composition (dotted line in Figure 5). For mass fractions of C_8E_3 in solution below $\delta = 24\%$, the mixed micelle at

(21) Holland, P. M. In *Mixed Surfactant Systems*; Holland, P. M., Rubingh, D. N., Eds.; American Chemical Society: Washington, DC, 1992; Vol. 501.

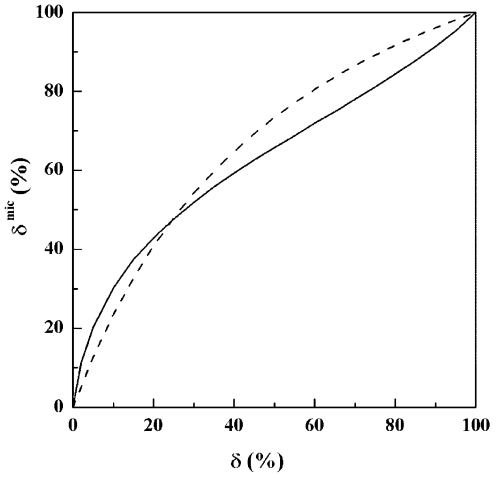

Figure 5. Micelle composition at cmc for mixtures of $C_8\beta G_1$ and C_8E_3 in water at 15 °C vs solution composition according to regular solution theory with $\beta = -1.0$. The dotted line is the prediction for ideal mixing ($\beta = 0$).

the cmc of the mixture is richer in C_8E_3 than in the ideal mixing case, whereas for δ above 24% the opposite trend is observed and micelles are leaner in C_8E_3 than the ideal mixing predicts. Furthermore, the mixed micelle composition as a function of total surfactant concentration (C) in solution can be calculated with an iterative procedure using the expressions

$$C_i^{mic} = C x_i - C_i^{mon} \tag{7}$$

$$C_1^{mon} = \frac{-(C - \Delta) + \sqrt{(C - \Delta)^2 + 4C x_1 \Delta}}{2\dfrac{\Delta}{f_1(x_1^{mic})\mathrm{cmc}_1}} \tag{8}$$

$$C_2^{mon} = \left(1 - \frac{C_1^{mon}}{f_1(x_1^{mic})\mathrm{cmc}_1}\right) f_2(x_2^{mic})\mathrm{cmc}_2 \tag{9}$$

$$\Delta = f_2(x_2^{mic})\mathrm{cmc}_2 - f_1(x_1^{mic})\mathrm{cmc}_1 \tag{10}$$

with f_1 and f_2 as functions of the micelle composition (eqs 2 and 3). The change in micelle composition with total surfactant concentration is more pronounced in mixtures with small δ (Figure 6). For all mixtures, the mixed micelle composition reaches the equilibrium bulk value at a surfactant concentration of approximately 10 times the cmc. It is worth noting that the error in the mixed micelle composition as a result of the experimental error in the evaluation of the interaction parameter is 0.5% or less.

Neutron Scattering of $C_8\beta G_1/C_8E_3$ Mixtures near the Cloud Point. Small-angle neutron scattering experiments were performed on mixtures of $C_8\beta G_1$ and C_8E_3 in a buffered D_2O solution at pD 6.5 and a background salt concentration of 0.5 M NaCl and 0.1 M Na_2HPO_4/NaH_2PO_4 (on a surfactant-free basis). Scattering experiments were performed at temperatures and total surfactant concentrations (γ) on paths approaching the cloud-point curve of the mixed surfactant system. Table 1 reports the cloud-point temperatures for the surfactant mixtures used in the experiment. Because of the additional shift of the solution transition temperature due to the substitution of H_2O by D_2O, for the scattering experiments mixtures with $\delta = 35$ and 40% were chosen so that the solution microstructure could be studied as a function of distance from the cloud point in the temperature range of 15 to 30

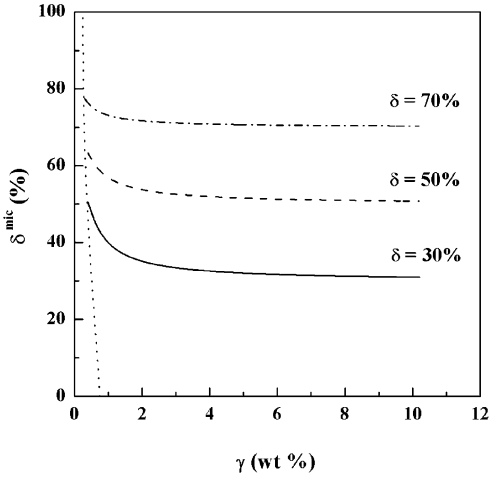

Figure 6. Micelle composition as a function of the total surfactant concentration for mixtures of $C_8\beta G_1$ and C_8E_3 in water at 15 °C according to the regular solution theory with $\beta = -1.0$. The dotted line on the left is the cmc line.

Table 1. Cloud Points of Surfactant Mixtures $C_8\beta G_1/C_8E_3$ in D_2O Buffered Solution with 0.5 M Sodium Chloride and 0.1 M Sodium Phosphate at pD 6.5

δ (%)	γ (wt %)	cloud point T_c (°C)
35	1.0	27.5
	3.0	31.1
	5.0	32.2
40	1.0	22.0
	3.0	24.8
	5.0	25.6

°C. The choice of the temperature range was based on practical aspects of protein crystallization experiments that are generally conducted at room temperature or below to avoid protein denaturation. The cmc of the $C_8\beta G_1/C_8E_3$ mixture with $\delta = 35\%$ in the buffered salt solution was determined to be 8.4 mM by surface tension measurement.

Figure 7a shows the neutron scattering profiles (after subtraction of the scattering from the background and the buffer solution) of $C_8\beta G_1/C_8E_3$ mixtures with fixed $\delta = 35\%$ and $\gamma = 1$ wt % while varying the temperature. As temperature increases toward the cloud-point curve, the forward-neutron-scattered intensity increases in the low-q range, whereas curves overlap for large q values. This suggests that the small dimension of the colloidal particle in solution (which sets the scattering at large q values) is maintained as temperature is increased, whereas there is an increase in either attractive interactions or the larger micelle dimensions of the aggregates (which sets the scattering at small q values) upon approaching the surfactant phase boundary. The same trend holds for mixtures with $\gamma = 3$ and 5 wt % with increasing temperature. Figure 7b shows scattering data for mixtures with fixed $\delta = 35\%$ and varying γ at 25 °C. The results are similar in that as the solution conditions approach the cloud-point curve small length scales are maintained, whereas larger length scales change. Similar results hold for $\delta = 35$ and 40%.

To gain quantitative insight into the microstructure of the $C_8\beta G_1/C_8E_3$ solutions at conditions near the phase boundary, the small-angle neutron scattering data were first evaluated using the indirect Fourier transformation (IFT) technique.[7,22] This evaluation procedure, introduced by Glatter, is a model-independent method to determine

(22) Glatter, O. *J. Appl. Crystallogr.* **1980**, *13*, 577−584.

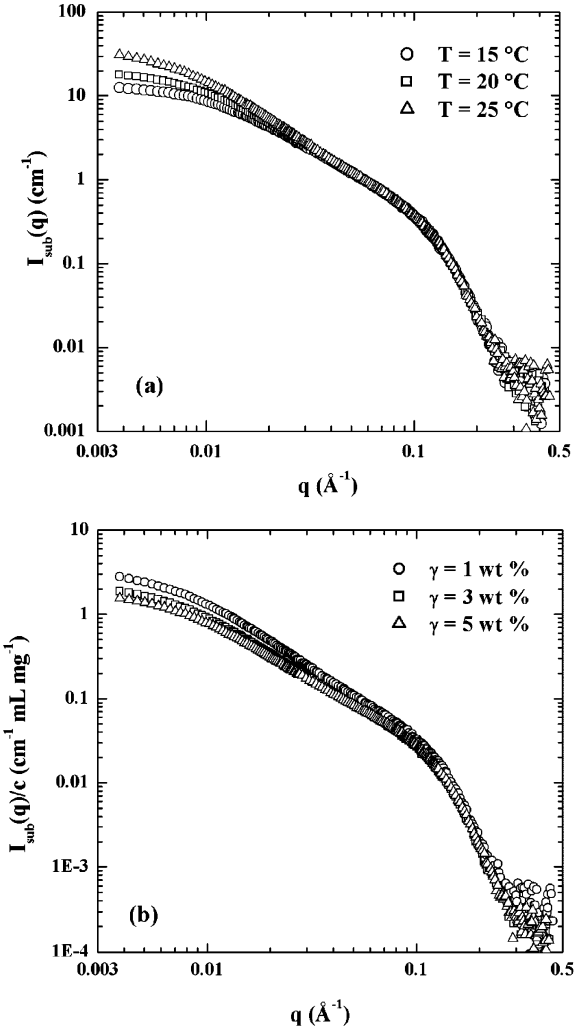

Figure 7. Scattering profiles of $C_8\beta G_1/C_8E_3$ mixtures with $\delta = 35\%$ and $\gamma = 1$ wt % at different temperatures (a) and mixtures with $\delta = 35\%$ and different γ's at a temperature of 25 °C (b).

the pair distance distribution function of particles in solution without knowledge of their shape. The scattering intensity is related to the pair distance distribution function $p(r)$ by the Fourier transformation

$$I(q) = 4\pi\int_0^\infty p(r)\frac{\sin(qr)}{qr}\,dr \qquad (11)$$

In the IFT method, the $p(r)$ function is approximated by a linear combination of a finite number of cubic B splines $\varphi_i(r)$

$$p(r) = \sum_{i=1}^{N} c_i\varphi_i(r) \qquad (12)$$

where the expansion coefficients c_i are the unknowns determined through a weighted least-squares fitting with the experimental data. The functions $\varphi_i(r)$ are defined in the range $0 \le r \le D_{max}$ where D_{max} is an estimate of the upper limit for the largest particle dimension and is limited by the lowest q value accessible in the scattering experiment $D_{max} \le \pi/q_{min}$. The IFT analysis can be extended to include effects due to interparticle interactions using the generalized indirect Fourier transformation (GIFT).[8,23]

Under the decoupling approximation,[24] the total scattering intensity $I(q)$ can be written as the product of the

form factor $P(q)$, which represents contribution to the scattered intensities from the particle geometry, and the structure factor $S(q)$, with the contribution from interparticle interactions

$$I(q) = n_p P(q)\, S(q) \tag{13}$$

where n_p is the number density of particles in solution. The GIFT method allows the simultaneous determination of both the form factor and the structure factor without assuming a model for the shape of the particles (i.e., a functional form for$P(q)$). For the structure factor, we used the modified Ornstein−Zernike model function

$$S(q) = 1 + \frac{n_p k_B T \chi_T}{1 + q^2 \xi_c^{\,2}} \tag{14}$$

where χ_T is the isothermal compressibility, ξ_c is the correlation length of the local concentration fluctuations, k_B is the Boltzmann constant, and T is the absolute temperature. χ_T and ξ_c are adjustable parameters determined through the GIFT procedure. The choice of this model for the structure factor was based on the experimental observation that samples do not show an increase in viscosity while approaching the cloud point, so the increase in scattering at low q can likely be attributed to critical scattering. Dynamic light scattering measurements were also performed showing an increase in the apparent size of the mixed micelles as solution conditions move closer to the cloud point. However, this increase can be due to critical scattering and/or to micelle elongation.

The GIFT analysis was repeated assuming different models for the structure factor (polydisperse hard spheres in the Percus−Yevick approximation and polydisperse cylinders), resulting in a larger mean deviation than the evaluation with the modified Ornstein−Zernike model. Scattering data were also analyzed by direct fitting assuming elongated aggregates with variable length and radius equal to the surfactant length. This model failed to fit the data at low q for solutions closer to the cloud point because scattering data do not display the q^{-1} dependence expected for cylindrical scatterers at lower q values, thus excluding the hypothesis that the increase in scattering at low q can be ascribed to micelle elongation.

Figure 8 shows the pair distance distribution function $p(r)$ from the IFT analysis for $C_8\beta G_1/C_8E_3$ mixtures with fixed $\delta = 35\%$ and varying temperature at total surfactant concentrations of 1 and 5 wt %. All profiles are characterized by a second peak that becomes noticeably larger as the temperature increases to the cloud point, whereas the position of the first peak stays the same. The second large peak can be ascribed to the strong interactions driven by the critical fluctuations near phase boundaries. For the surfactant mixtures in this study, such fluctuations extend as far as 20 °C below the cloud temperature, as also evident from the presence of the second peak in solutions with $\gamma = 5$ wt % at 15 °C ($T_c = 32.2$ °C). Because of experimental limitations, lower temperatures, at enough distance from the boundary where critical fluctuations are negligible, could not be examined.

To quantify the critical fluctuations and at the same time extract information on the micellar size, we applied the GIFT method with the hypothesis described above. Figure 9 shows the $p(r)$ normalized by the total surfactant concentration for the same $C_8\beta G_1/C_8E_3$ mixtures after the contribution of the attractive micellar interactions driven by the concentration fluctuations near phase boundary was separated from the geometric features of the micelles with the GIFT procedure. The normalized $p(r)$ functions from GIFT for all of the solutions studied are similar and show only one peak with comparable height positioned at the same value of r. The shape and symmetry around the peak indicate that $C_8\beta G_1/C_8E_3$ mixtures with $\delta = 35\%$ form globular micelles in solution for γ values ranging from 1 to 5 wt % and at all temperatures studied. The micelles have a slightly elongated shape, with a maximum dimension that corresponds to the point where $p(r)$ decays to zero of about 55 Å. The minimum dimension of the micelles was estimated to be 35 Å from the first point of inflection after the maximum value of $p(r)$. This value corresponds to a minor radius of 17.5 Å, which is in agreement with the overall surfactant length calculated as the sum of the octyl carbon chain length (11.7 Å) and a headgroup diameter of 6.5 Å, calculated from an average headgroup area based on the composition of the mixed micelle at $\delta = 35\%$ and $\gamma = 1$ wt %. The E_3 headgroup area (25.7 Å^2) was calculated from available correlations for

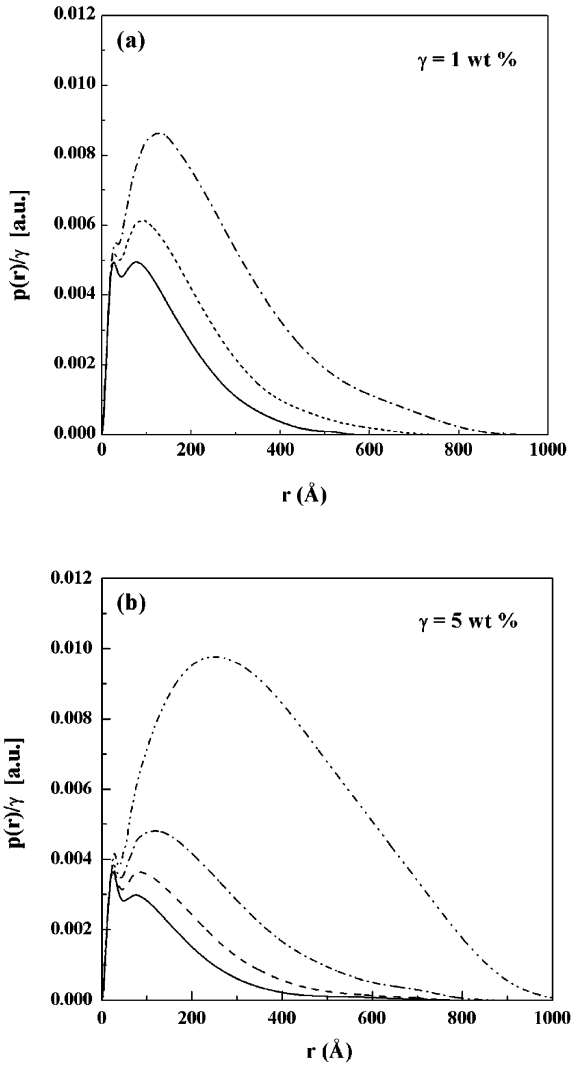

Figure 8. Pair distance distribution function from IFT analysis normalized by total surfactant concentration for $C_8\beta G_1/C_8E_3$ mixtures ($\delta = 35\%$) and $\gamma = 1$ wt % (a) and 5 wt % (b) at temperatures of 15 (—), 20 (- - -), 25 (·-·-·), and 30 °C (··-··-).

(23) Glatter, O.; Fritz, G.; Lindner, H.; Brunner-Popela, J.; Mittelbach, R.; Strey, R.; Egelhaaf, S. U. *Langmuir* **2000**, *16*, 8692−8701.
(24) Kotlarchyk, M.; Chen, S. H. *J. Chem. Phys.* **1983**, *79*, 2461−2469.

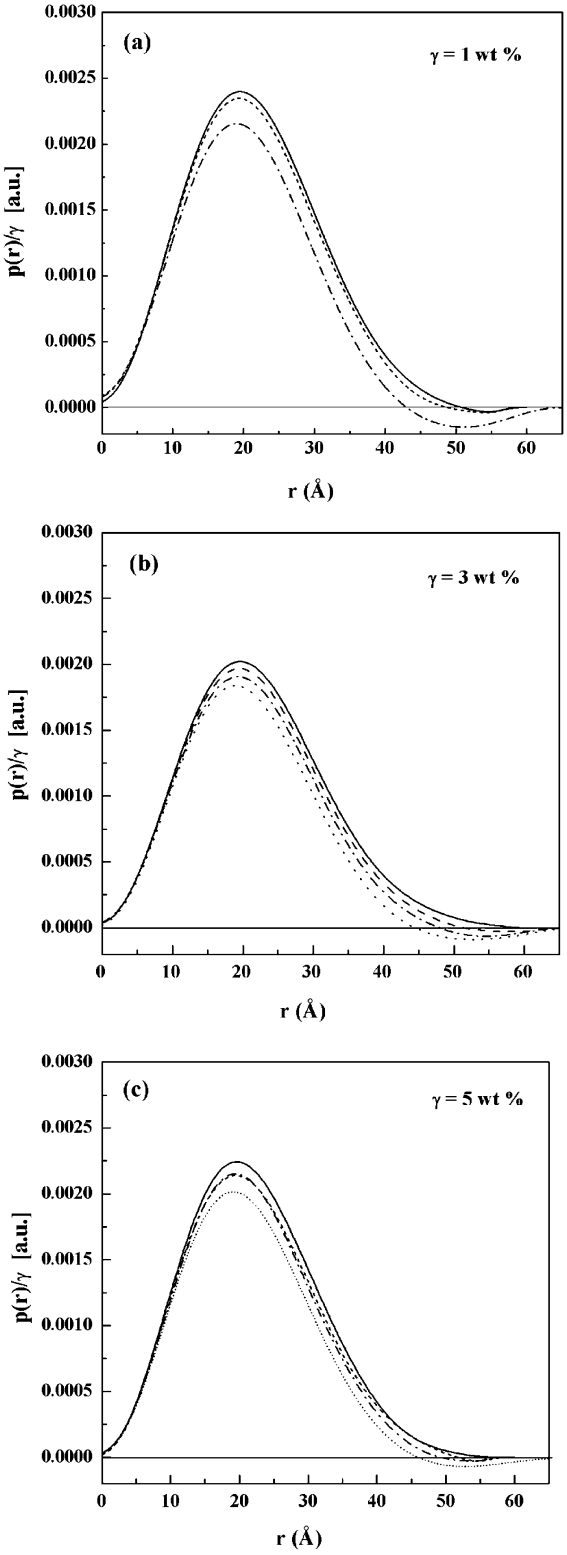

Figure 9. Pair distance distribution function from GIFT analysis normalized by total surfactant concentration for $C_8\beta G_1/C_8E_3$ mixtures with $\delta = 35\%$ and $\gamma = 1$ wt % (a), 3 wt % (b), and 5 wt % (c) at temperatures of 15 (—), 20 (- - -), 24 (·-·-·), and 30 °C (···).

C_iE_j surfactants,[25] whereas the glucose headgroup area (40 Å^2) was estimated from the densities of glucose solutions.[9]

The shape and the dimensions of the mixed micelles were verified by direct fitting of the scattering profiles with a uniform ellipsoid model for the particle form factor and a structure factor of the modified Ornstein−Zernike type. Mixed micelles can be well approximated as prolate ellipsoids with the rotational axis equal to the maximum dimension obtained through the GIFT analysis and a minor radius of about 16 Å. The most important result from the GIFT analysis is that these mixed micelles do not show a significant change in size and shape for total surfactant concentrations in the range of 1 to 5 wt % and do not grow upon approaching cloud-point conditions. These conclusions agree with previous scattering studies of C_8E_4 and C_8E_5 in D_2O.[13,26]

Both the isothermal osmotic compressibility, χ_T, and the correlation length of concentration fluctuations, ξ_c, of mixtures with 1, 3, and 5 wt % total surfactant concentration diverge as a function of the reduced temperature, ϵ, defined as

$$\epsilon = \frac{T_c - T}{T_c} \tag{15}$$

which measures the distance of the solution condition from its cloud point (Figure 10). The temperature dependence of the parameters χ_T and ξ_c is described by

$$\chi_T = \chi_{T0}\epsilon^{-\Gamma} \tag{16}$$

$$\xi_c = \xi_0\epsilon^{-\nu} \tag{17}$$

where Γ and ν are critical exponents that can be determined by least-squares fitting of the experimental data. The values of Γ and ν depend on the value of γ, with $\Gamma = 0.82$ and $\nu = 0.31$, respectively, for $\gamma = 1$ wt %; 0.97 and 0.47, respectively, for $\gamma = 3$ wt %; and 1.26 and 0.61 for the $\gamma = 5$ wt % surfactant solution. The values of exponents Γ and ν for the 5 wt % solution are in agreement with the predicted Ising universal values. Similar exponents have been reported previously for solutions of $C_{12}E_8$ in D_2O near the lower consolute point.[26] However, upon decreasing γ from 5 to 1 wt %, Γ and ν become significantly smaller. Such deviations have been observed for asymmetric liquid−liquid phase boundaries because the critical concentration path does not coincide with the maximum compressibility path.[27,28] $C_8\beta G_1/C_8E_3$ mixtures are characterized by asymmetric phase boundaries. For mixtures of surfactants, this asymmetry can be explained by the observation that there is a range of surfactant concentration where micelles change composition before reaching the bulk composition. In the case of $C_8\beta G_1/C_8E_3$ mixtures with $\delta = 35\%$, the mixed micelles at a surfactant concentration of 1 wt % are enriched in C_8E_3 ($\delta^{mic} = 43\%$), which is the more hydrophobic component, with respect to the solution composition. The micelle composition approaches the bulk value at ~3 wt %. Such a change in composition and the consequent change in the micelle−solvent interaction can account for the asymmetry of the phase boundaries and the consequent variations of exponents Γ and ν with surfactant concentration. Equilibration problems due to the presence of impurities can be excluded as the reason for such variations because they affect the determination of the lower consolute point only for solutions with a surfactant concentration equal to the cmc (0.3 wt % for mixtures with $\delta = 35\%$ in the D_2O buffer used for the scattering experiments) or lower.

(25) Nikas, Y. J.; Puvvada, S.; Blankschtein, D. *Langmuir* **1992**, *8*, 2680−2689.

(26) Corti, M.; Degiorgio, V. *Phys. Rev. Lett.* **1985**, *55*, 2005−2008.
(27) Corti, M.; Degiorgio, V. *Phys. Rev. Lett.* **1980**, *45*, 1045−1048.
(28) Corti, M.; Degiorgio, V.; Zulauf, M. *Phys. Rev. Lett.* **1982**, *48*, 1617−1620.

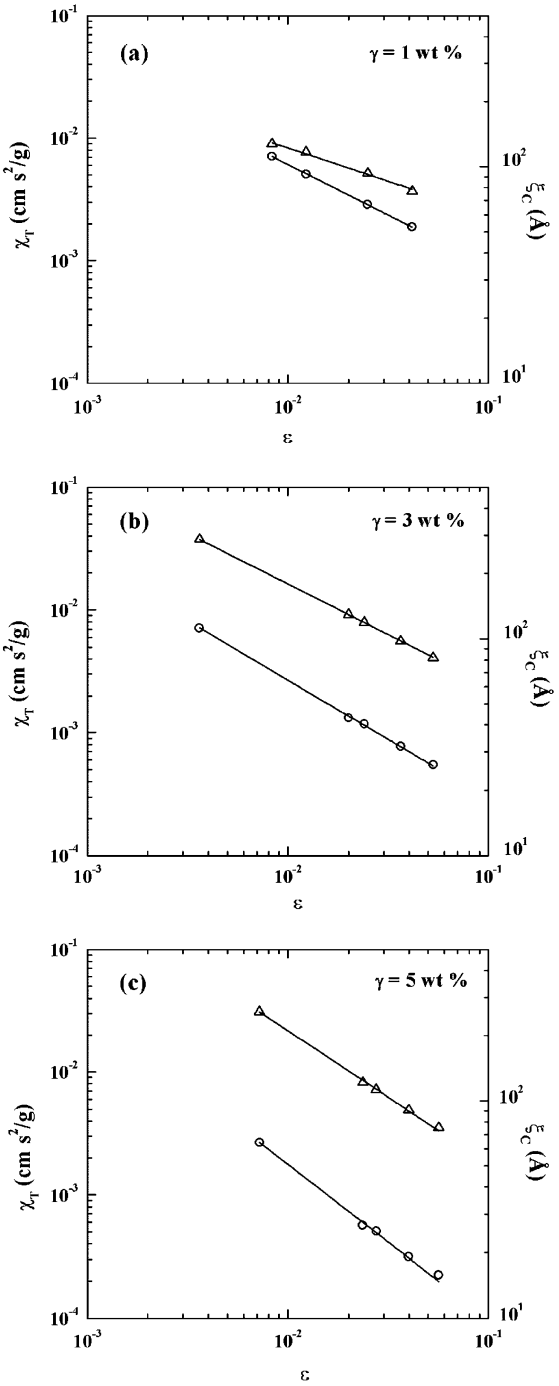

Figure 10. Isothermal osmotic compressibility (○) and correlation length (△) of concentration fluctuations vs reduced temperature for $C_8\beta G_1/C_8E_3$ mixtures with $\delta = 35$ wt % and $\gamma = 1$ wt % (a), 3 wt % (b), and 5 wt % (c). The solid lines are the power-law fits to the data.

The number of surfactant monomers per aggregate (or aggregation number) can be calculated from the total surfactant concentration once the number of aggregates in solution is known. The number density of micelles was estimated from

$$n_p = \frac{\phi - \phi_{cmc}}{V_p} \tag{18}$$

where ϕ is the surfactant volume fraction and V_p is the volume of the micellar aggregate, which is assumed to be a prolate ellipsoid with dimensions obtained from the GIFT analysis above. The aggregation number of $C_8\beta G_1/C_8E_3$ micelles with $\delta = 35\%$ at 15 °C is 78 for a surfactant concentration of $\gamma = 1$ wt %, and it increases to 91 and 92 for $\gamma = 3$ and 5 wt %, respectively. Such an increase can be explained by the fact that micelles at $\gamma = 3$ and 5 wt % are richer in $C_8\beta G_1$, which has a more compact headgroup than C_8E_3 and can pack more efficiently in the mixed micelle.

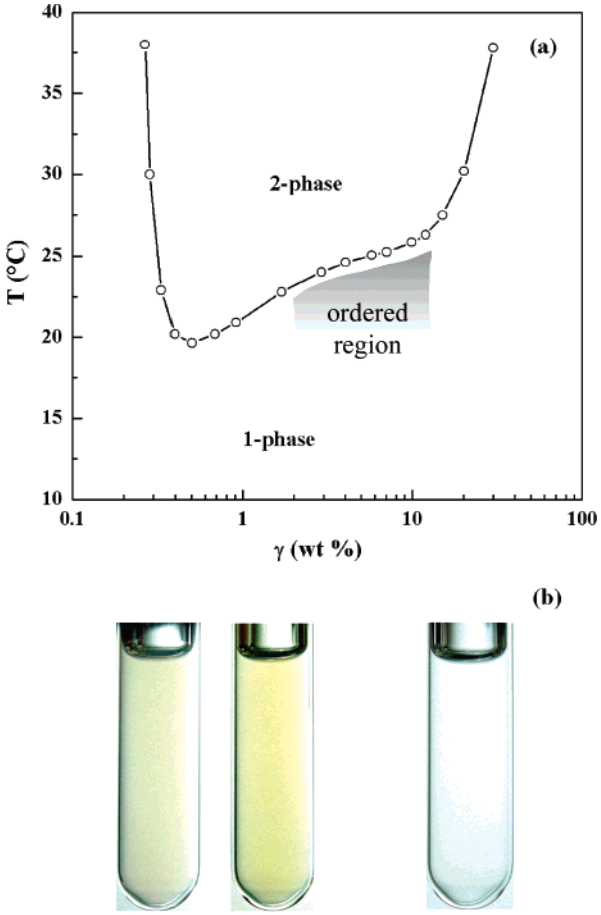

Figure 11. (a) Schematic of the ordered region for colloidal silica in $C_8\beta G_1/C_8E_3$ mixtures ($\delta = 70\%$) in 50 mM NaCl buffer solution at pH 9.0. (b) Surfactant solution ($\gamma = 5$ wt %) with a 0.025 volume fraction of 22 nm silica particles after 24 and 48 h at 22 °C (left) and silica-free surfactant solution (right).

Colloidal Silica Ordering near the Cloud Point of $C_8\beta G_1/C_8E_3$ Mixtures. The behavior of colloidal silica spheres dispersed in $C_8\beta G_1/C_8E_3$ mixtures is strongly affected by their proximity to the liquid−liquid phase boundary. To avoid particle aggregation due to changes in ionic strength, the background solution of the colloidal silica was kept at 50 mM ionic strength (by NaCl) and at pH 9 as supplied by the manufacturer. Surfactant cloud points were measured in such aqueous buffer before adding silica particles. Figure 11a shows the surfactant phase boundary for mixtures with $\delta = 70\%$. Because of the addition of NaOH to increase the pH to 9, the miscibility boundary is shifted upward by about 5 °C. A similar shift of the cloud point as a result of NaOH addition, in contrast with the downward shift induced by NaCl, has been previously observed for solutions of alkyl polyglucosides.[18] Silica particles in the concentration range of 0.5 to 5 wt % were added, and solutions were examined at different temperatures approaching the cloud point. Solutions with colloidal silica were a bright orange color that became more intense with time (Figure 11b), indicating the formation of aggregates of silica particles with time.

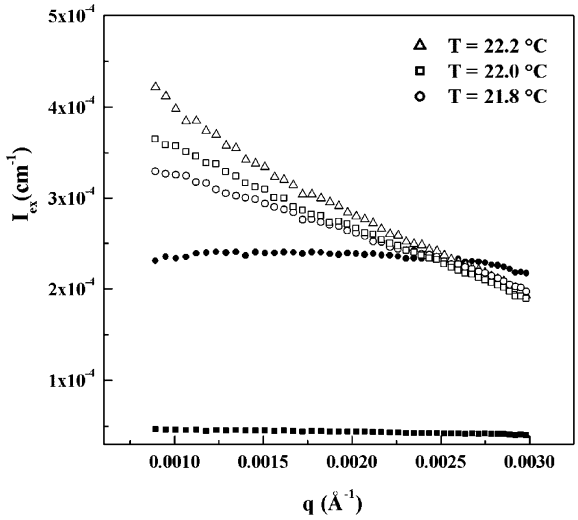

Figure 12. Static light scattering from 22 nm silica particles (0.025 volume fraction) in $C_8\beta G_1/C_8E_3$ solution ($\delta = 70\%$, $\gamma =$ 5 wt %) in 50 mM NaCl buffered solution at pH 9.0 at different temperatures. Full symbols represent the surfactant-free particle solution (●) and the silica-free surfactant solution (■) at $T = 22$ °C.

However, no dependence of color on the angle of observation, as previously reported for polystyrene particles,[1] was observed because of the small size of the particles used here (22 nm). To characterize the extent of this aggregation near the cloud point, static light scattering experiments were performed on $C_8\beta G_1/C_8E_3$ solutions ($\delta = 70\%$ and $\gamma = 5$ wt %) before and after the addition of silica particles (0.025 volume fraction) as T increased toward the cloud point of the surfactant solution (24.8 °C). Figure 12 shows the normalized scattered intensities plotted as a function of scattering vector q at different temperatures. The increase in scattering at small q observed over a small temperature change (less than 1 °C) suggests that particle aggregation near phase boundaries can be tuned by small changes in the solution conditions. Analogous small changes in solutions conditions affect protein crystallization and crystal quality. It is widely observed in fact that well-ordered crystallization of proteins occurs only in a small window of solution conditions.[29,30] Although the nature of the interactions in this window appears clear, that is, weakly attractive interactions induced by concentration fluctuations in the proximity of a phase-transition point, its exact location appears to be system-dependent and is difficult to predict. The values of the isothermal osmotic compressibility for the $C_8\beta G_1/C_8E_3$ mixtures reported in Figure 10 show that solutions with the same reduced distance from the cloud point are characterized by attractive interactions with different strengths. Moreover, the change in the osmotic compressibility while solution conditions approach the cloud point depends on the total surfactant concentration. In a solution with 5 wt % total surfactant concentration, interactions change rapidly with temperature. These results can help explain the large variations in static light scattering patterns observed in solutions with silica particles over the small temperature range.

Conclusions

The micellar properties of $C_8\beta G_1$ in water can be tuned by the addition of C_8E_3, a medium-strength amphiphile. The combination of such surfactants shows synergism, so the addition of small amounts of C_8E_3 to $C_8\beta G_1$ solutions induces a cloud-point phenomenon at low surfactant concentration. The addition of salt to the surfactant mixture further reduces the cloud-point boundary. Mixed micelles in solutions of $C_8\beta G_1$ and C_8E_3 close to the cloud point do not grow, whereas the attractive interactions between micelles become progressively stronger while approaching the cloud point. These mixtures are characterized by strong concentration fluctuations at temperatures from 20 to 2 °C below the phase boundary. Such results have strong implications for the stability of colloid and protein solutions and can be used as guide toward a rational manipulation of their macroscopic behavior.

Acknowledgment. We acknowledge the support of the National Institute of Standards and Technology, U.S. Department of Commerce, in providing the neutron research facilities used in this work, which were supported in part by the National Science Foundation under agreement no. DMR-9986442. Funding from NASA through grant NAG8-1830 is gratefully acknowledged.

LA050573V

(29) Garavito, R. M.; Picot, D.; Loll, P. J. *J. Bioenerg. Biomembr.* **1996**, *28*, 13−27.

(30) George, A.; Wilson, W. W. *Acta Crystallogr., Sect. D* **1994**, *50*, 361−365.